LASER INTERFEROMETER GRAVITATIONAL WAVE OBSERVATORY
- LIGO -
CALIFORNIA INSTITUTE OF TECHNOLOGY
MASSACHUSETTS INSTITUTE OF TECHNOLOGY

Technical Note	**LIGO-T1400252-LSC**	2014/05/03

Imaging Scatterometer Characterization of Advanced LIGO Optic ITM06

Adrian Avila-Alvarez, Garilynn Billingsley, Joshua Hacker, Joshua Smith, Daniel Vander-Hyde, Liyaun Zhang

California Institute of Technology
LIGO, MS 100-36
Pasadena, CA 91125
Phone (626) 395-2129
Fax (626) 304-9834
E-mail: info@ligo.caltech.edu

Massachusetts Institute of Technology
LIGO, NW22-295
Cambridge, MA 02139
Phone (617) 253-4824
Fax (617) 253-7014
E-mail: info@ligo.mit.edu

LIGO Hanford Observatory
PO Box 159
Richland, WA 99352
Phone (509) 372-8106
Fax (509) 372-8137
E-mail: info@ligo.caltech.edu

LIGO Livingston Observatory
19100 LIGO Lane
Livingston, LA 70754
Phone (225) 686-3100
Fax (225) 686-7189
E-mail: info@ligo.caltech.edu

http://www.ligo.caltech.edu/

1 Introduction

In this document we report on the scatter characteristics of the Advanced LIGO test mass ITM06 [1, 2]. After it was coated by the vendor LMA, the vendor characterization found that the Anti-Reflective (AR) coating showed a cloudy or leopard-print scattering pattern when seen under visible light, but that its scattering BRDF values were reasonably low [3]. We performed an imaging scatterometer characterization of the AR-coated surface in order to confirm the LMA measurements and provide more information about the spatial character of the scatter, particular the impact of the leopard pattern when illuminated by 1064 nm light, the primary wavelength of light used in the Advanced LIGO interferometers. We find that ITM06 does have an abnormal anti-reflection coating and we present images of the leopard pattern illuminated by low levels of 1064 nm light. However, we find that the scatter level, while higher than that from other AR-coated optics [4], appears to be low enough (similar to LMA's measurements) to be suitable for use in Advanced LIGO.

In Advanced LIGO, Input Test Masses are used as highly-reflective input-coupling mirrors and, together with the End Test Masses (ETMs), form aLIGO's 4 km-long Fabry-Perot cavities. The role of the Fabry-Perot cavities is to build up the circulating light power, and to serve as an accurate length standard for control of the laser's frequency noise. The shot-noise-limited sensitivity of the aLIGO detectors scales roughly as the square-root of the circulating power, so optical loss due to scattered light can decrease aLIGO's sensitivity by decreasing the laser power in the Fabry-Perot cavities. In addition, scattered light can bounce off moving surfaces and re-enter the interferometer adding non-linear phase noise. These effects drive the requirements on scattered light for the HR and AR coatings of the ITMs. In this document, we focus only on the abnormal AR coating on ITM06.

2 Sample

The input test mass, ITM06, has one highly reflective (HR) and one anti-reflection coated surface. It weighs approximately 40 kg and is 200 mm thick with a width of 326 mm [1]. The AR coating on ITM06 has regions where a cloudy/leopard-print pattern appears, when viewed under bright visible light, as shown in Figure 3. We sought to measure whether this pattern increases the scatter at 1064 nm with respect to other AR coatings, and if so, whether the levels are tolerable for aLIGO.

3 Setup and Procedure

Figure 1 shows an image of the Fullerton Imaging Scatterometer (FIS) with ITM06 installed. Prior to these measurements, the optic was thoroughly cleaned using First Contact and a nitrogen and de-ionizing gun spray. Here we briefly describe that setup, although more complete descriptions can be found in References [4, 5].

ITM06 was mounted on a motorized rotation stage using a series of rails and clamps to ensure that the test mass would not move. These rails were parallel to the optic's surfaces, and stretched as far as the width of the optic. Base-like structures were installed on the rails

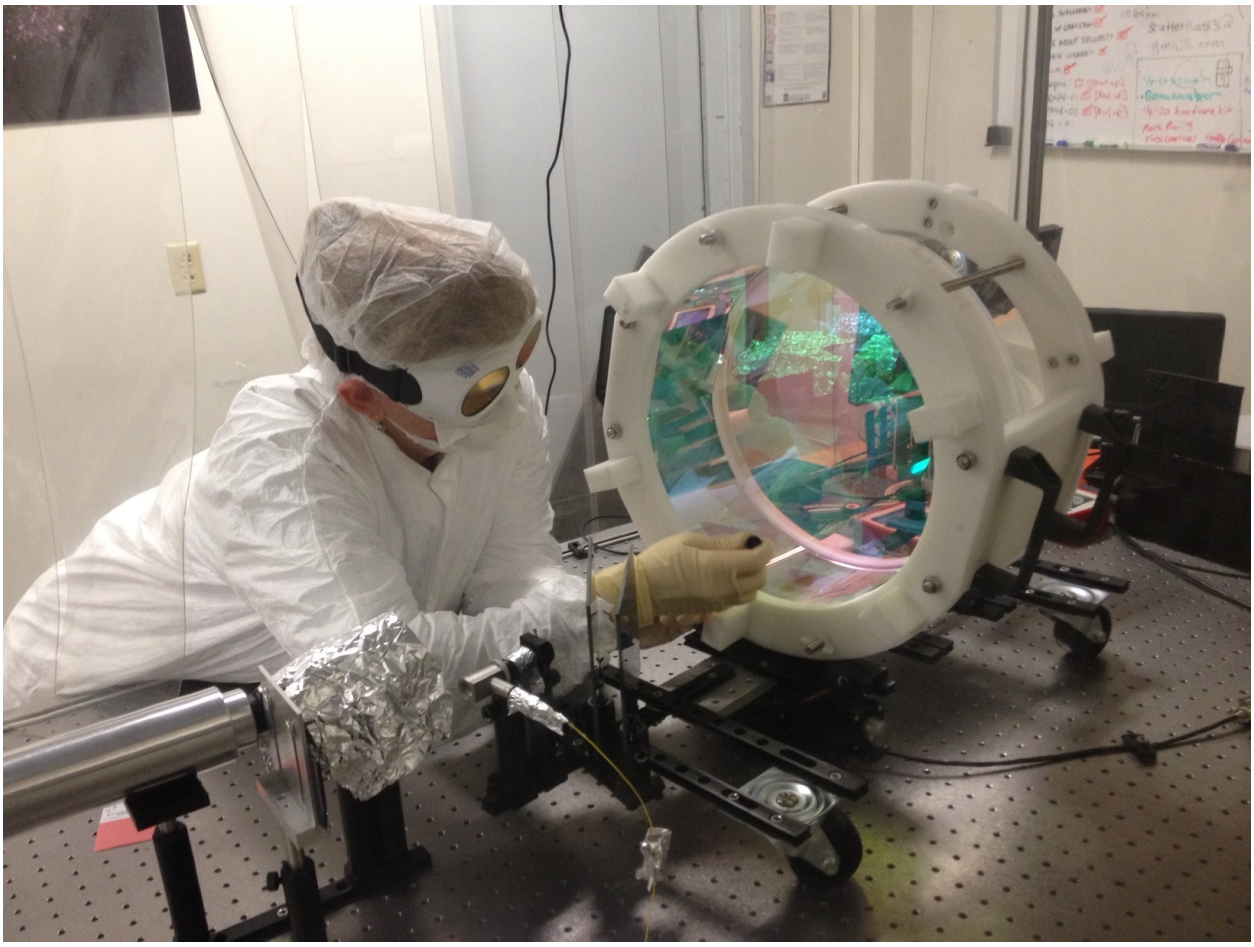

Figure 1: GariLynn applying a small amount of Frist Contact for the final cleaning that led to all of the measurements presented here. ITM06 is in its protective handling case and mounted on top of a motorized rotation stage. The yellow fiber carries the laser to the setup, it is then collimated, and passed through a linear polarizer and iris before hitting the sample. Behind the laser launch is a lens and iris, then aluminum tube, followed by a CCD camera that makes the images.

and placed under the optic to avoid movement. Wheels were also installed on the rails to balance the torques on the rotation stage and to level the laser beam.

A fiber-coupled Innolight Mephisto 1064 nm laser was passed through a reflective collimator, linear polarizer, and iris (all on a rail nearly perpendicular to the optic surface), giving a fixed angle of incidence of 5 degrees onto ITM06's AR-coated surface. Black shade 10 welding glass was used to make a trap beam dump for the reflected beams and these were also attached to the rail system on the rotation stage so that beams would always be dumped as the stage rotated.

Approximately one square inch of the optical surface was imaged by a lens-iris system onto a CCD camera that was fixed to the table. Much care was taken to remove other sources of stray light so that the light imaged would be dominated by scatterd light from ITM06's AR-coated surface.

For measurements, the stage rotated in one degree increments, and a long exposure time (60 s) image was taken at each step. The laser beam angle of incidence is fixed on the optic's AR-coated surface, while a lens and iris are used to form an image of that surface on the CCD camera for each viewing angle. The CCD camera captures one image for each one-degree increment that the rotation stage moves. Then the laser is turned off and the procedure is repeated to collect a set of dark images that are subtracted from the original images to reduce noise. Finally, the images are processed using a custom-written MatLab script that applies a calibration, extracts the scattered power, and computes the Bidirectional Reflectance Distribution Function or BRDF [6]. The calibration factor that was applied to the images was verified by checking that we got the correct BRDF values for a well-understood viewport sample.

The CCD camera was exposed for 60 seconds at each viewing angle. This exposure time was the highest before saturation of the images occurred. Angles below about 7 degrees are not usable because the camera cannot see past our laser launching optics. Angles beyond 65 degrees were not usable because the ITM06's front surface could not be seen by the camera due to obscuration from its white protective holder. Our region of measurement and analysis was near an outer edge of ITM06 (the area GariLynn is cleaning in the photo).

The laser power was incident on the optic's surface with a power of 35.6 mW. Figure 2 shows the intensity distribution of the beam that was used by the imaging scatterometer when characterizing ITM06. It has a beam diameter of about 4 mm, which is from a slightly larger Gaussian beam, clipped by an iris. This shows that there is some unwanted light outside of the main beam, particular in the vertical direction.

4 Results

Figure 4 shows a 1"x1" region of the AR-coated surface of ITM06 imaged by our CCD camera at a scattering angle of 5 degrees. The black/white range (the minumum and maximum values set for black and white for the 16-bit color range shown in the image) is set to emphasize low levels of scatter. The spot on the left is the coating/surface backscatter from the incident light, the spot on the right is the coating/surface scatter from the re-transmitted

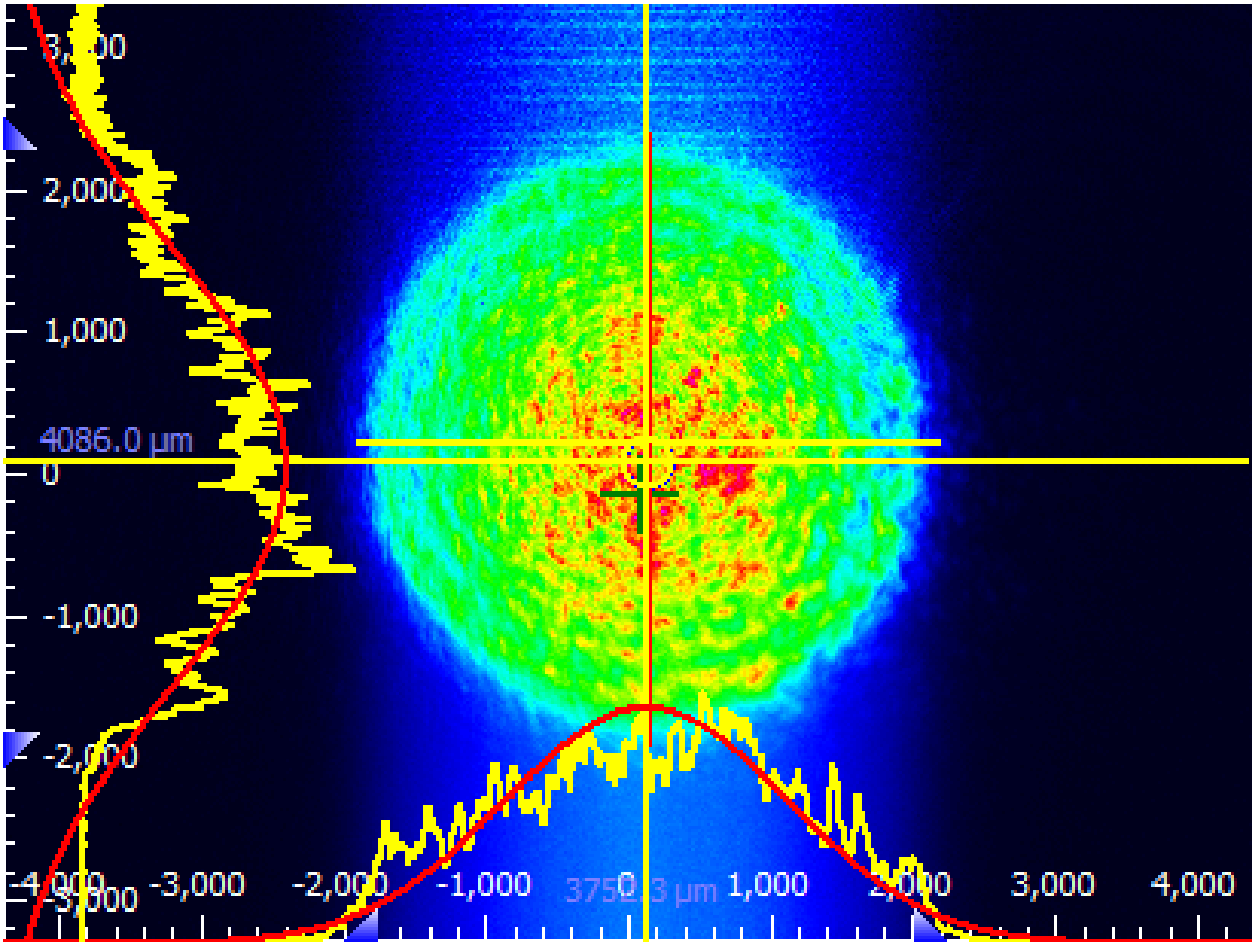

Figure 2: Intensity distribution of the incident laser beam used by the Fullerton Imaging Scatterometer, as measured using a Thorlabs BC106 Beam Analyzer.

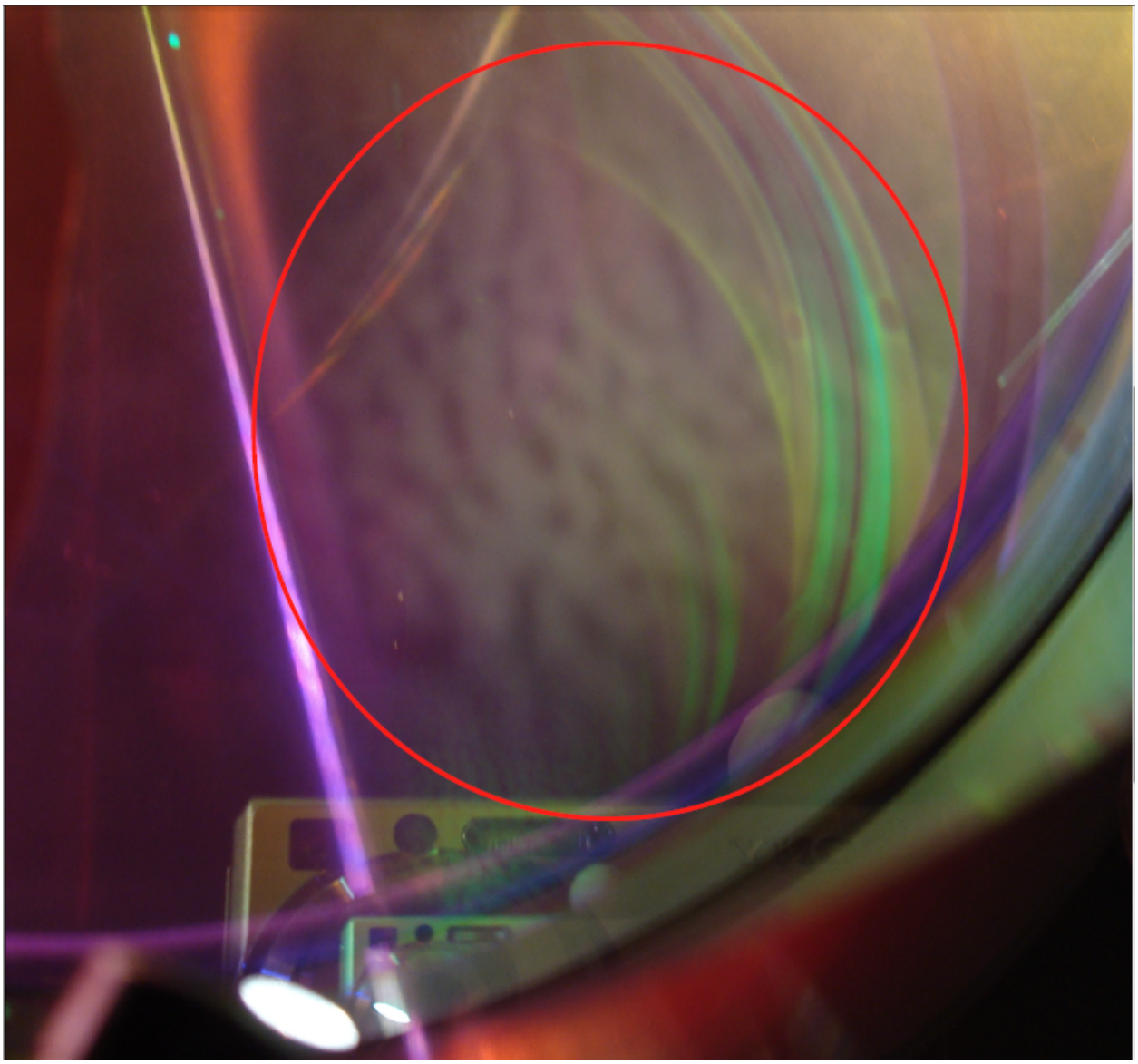

Figure 3: Image taken from Reference [3], showing the leopard pattern that is visible on the AR-coated surface in bright visible light.

light (after reflecting from the HR surface, not shown), the horizontal beam-shaped areas are Rayleigh (bulk) scattering from the beam passing through the fused silica substrate, and seen across the entire image is the leopard pattern, illuminated by the 1064 nm light.

Figure 5 shows the same image with the black/white range set such that the scatter characteristics of the incident and re-transmitted spots can more clearly be made out. The other bright pixels are hot pixels that are also present in the dark images and are subtracted in the image analysis and can be ignored.

Figure 6 shows a processed image (after dark image subtraction) for a scattering angle 30 degrees. Also shown are the different "Regions of Interest" (RoIs) that are used to calculate the enclosed scattered laser power, and from that, BRDF and TIS. Each RoI "follows" the beam spots (which move slightly because of imperfect centering over the rotation axis) and adjust their width with the cosine of the viewing angle in order to enclose the same area of the optic as the viewing angle changes. Movies of this process can be seen on the DCC page for this document.

Figure 7 shows the measured BRDF versus angle calculated from the images taken of ITM06, for each of the regions of interest shown in Figure 6. Several things can be seen from these data. Over the angles of about 8 degrees to 65 degrees, the data lie at least a factor of 3 above the image noise limit. The incident and re-transmitted beam spots have similar BRDF to each other (with differences potentially explainable by being on different parts of the leopard pattern - nodes or anti-nodes), but contain only a fraction of the total scatter. The 'Total Scatter' and 'Total Scatter Extended' regions look very similar to each other and the BRDF increases the more area is enclosed, meaning that the leopard-print pattern's scattering intensity is not negligible half an inch from the laser beam.

Table 1 shows the the total integrated scatter (TIS) of ITM06 for the incidence angle used, estimated by integrating the cosine-corrected BRDF over θ_s and ϕ_s, assuming independence of scatter on the azimuthal angle, following the steps described in Section 3 of Reference [5]. Note that this TIS is not really "total" because it is only over 1.12π steredians, corresponding to the measured polar scattering angles. The complete scatter is likely to be approximately double for the second direction, and some other small factor for missing the small angles. Safe to say, greater than 10 ppm.

Table 1: Integrated scatter estimates for the measured scattering angle range.

Region	θ_s Range	Solid Angle (sr)	Total Integrated Scatter (ppm)
Incident	10° - 64°	1.12π	1.07
Retransmitted	10° - 64°	1.12π	1.04
Total	10° - 64°	1.12π	3.53
Total (Extended Height)	10° - 64°	1.12π	5.14

5 Conclusions

From the analysis described above, we can draw several conclusions. Although the leopard-print pattern is visible under 1064 nm light, even far from the central beam, the scatter of

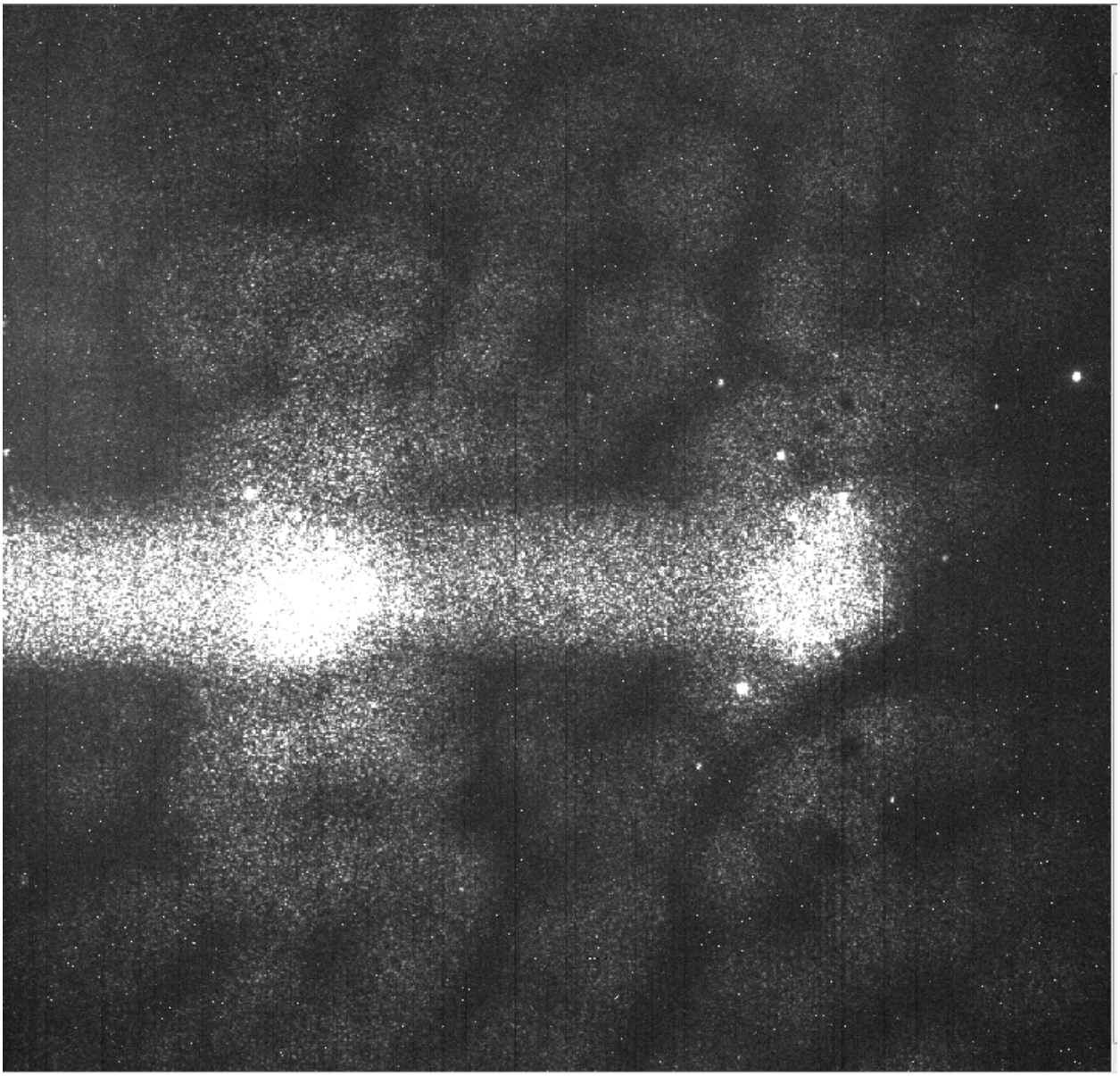

Figure 4: CCD image from the Fullerton Imaging Scatterometer showing the incident back-scattered spoot (left), the re-transmitted forward-scattered spot (right), the Rayleigh (bulk) scattering (beam regions), and that the leopard pattern is visible when illuminated by 1064 nm light.

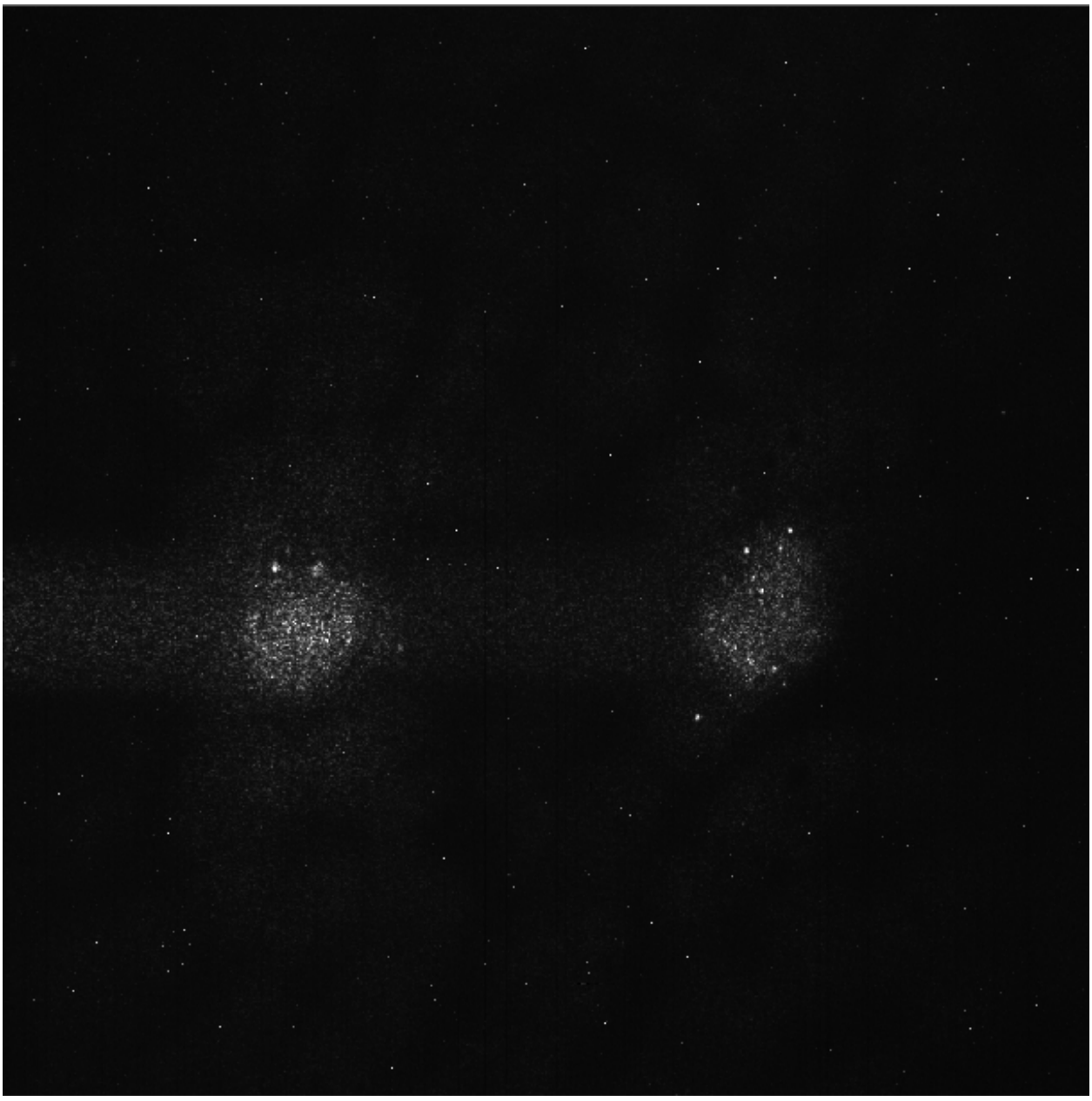

Figure 5: Same image as in Figure 4, except with black/white range set wider to more clearly see the character of the surface/coating scattering at the beam spots.

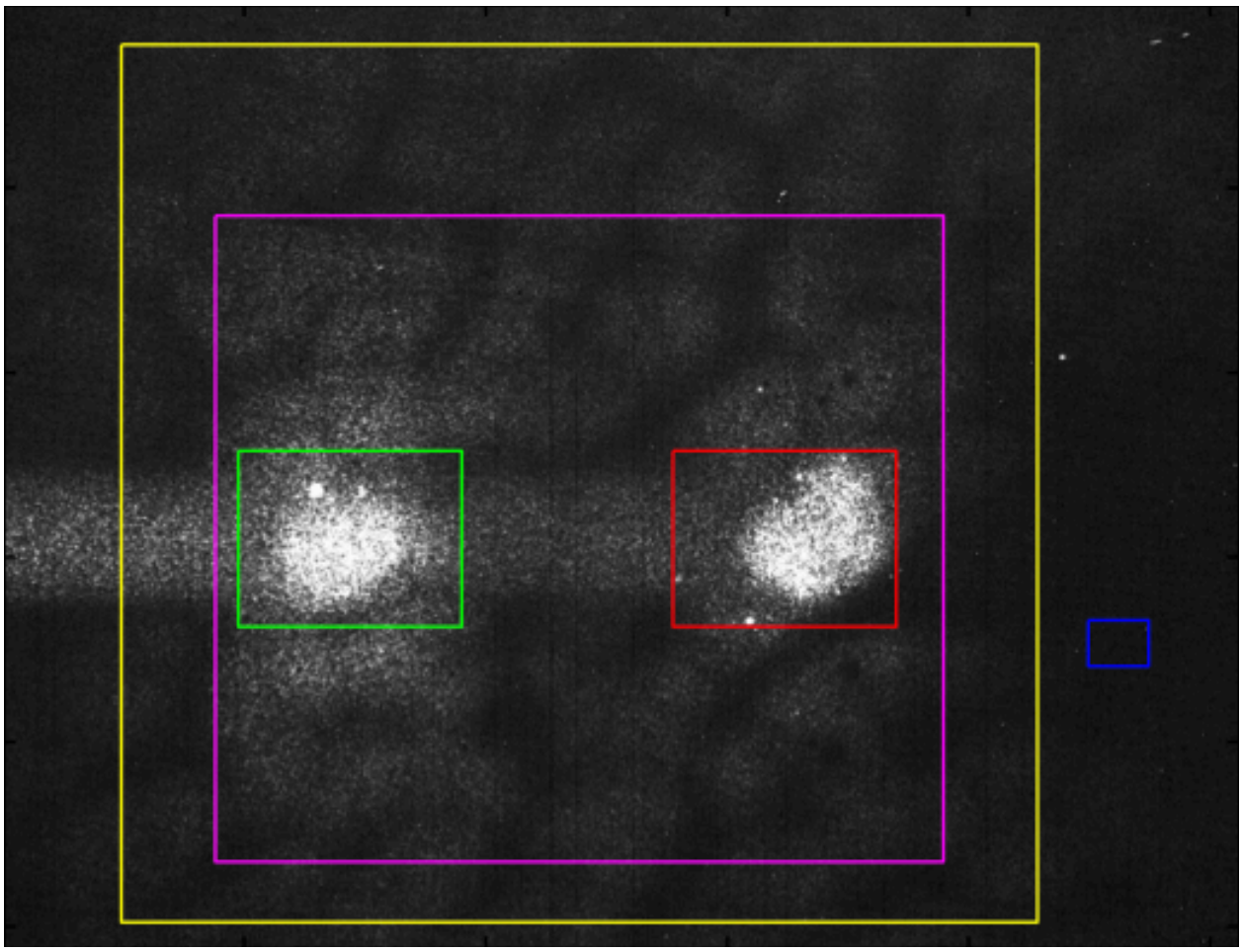

Figure 6: Each rectangle represents one Region of Interest (RoI), where we calculate the BRDF based on the imaged scattered light enclosed in that rectangle. The green RoI encloses the incident laser beam spot. The red RoI encloses the re-transmitted beam spot. The magneta RoI encloses both spots and some of the Rayleigh scattering and the leopard pattern. The yellow RoI, 'Total Scatter Extended', is similar to the last, but larger to include most of the scatter visible in the leopard pattern. Lastly, the blue RoI is a moving box that indicates the darkest 50x50 pixel region in the whole image. This is used to estimate our instrument background.

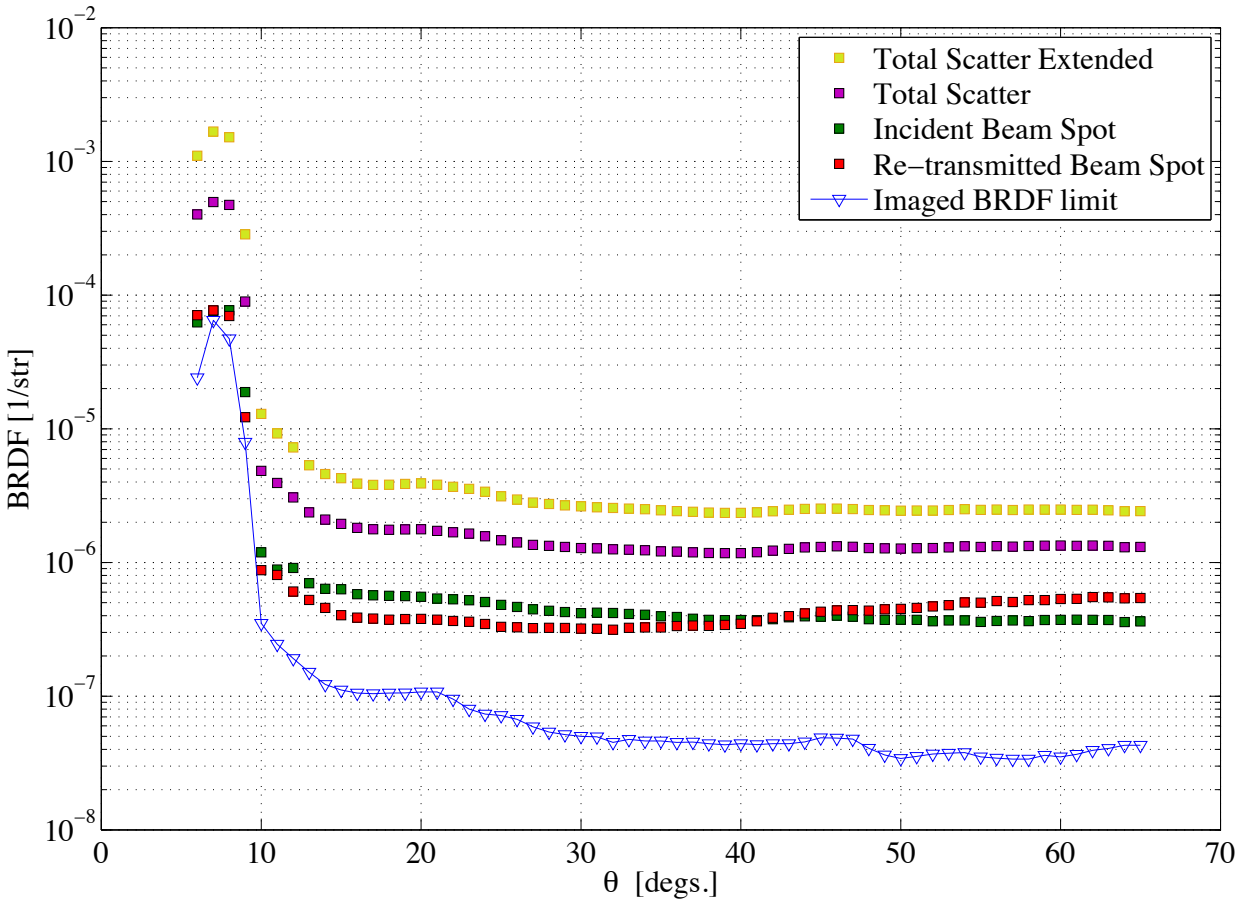

Figure 7: Plot of BRDF versus scattering angle for the different Regions of Interest on the AR-coated surface of ITM06 (color matched to Figure 6).

the ITM06 is surprisingly low. Both the incident beam and re-transmitted beam regions have nearly flat BRDF curves above 10° between 1e-6 and 4e-7 str $^{-1}$. These BRDF values are similar to or somewhat higher than (for largest RoIs) the LMA results. The region containing both spots and the leopard pattern are 5-10 times higher than that - but still not disastrous.

In addition, the beam that we used had an intensity that did not fall off exponentially from the center (Gaussian Beam). As was shown in Figure 2, we had a significant amount of light outside of the main beam spot, particularly in the vertical direction. This partially explains why the leopard pattern is seen so brightly in our images.

We also have some weak evidence that the scattering from the incident and re-transmitted beam spots depends on where it was located within the leopard background. The leopard-print pattern was capable of increasing the brightness of a spot, and therefore increasing the scatter as measured by our instrument. We came across this issue when we first noticed that the re-transmitted beam spot was brighter than the incident beam spot. Later, when we moved the optics, the incident beam spot became slightly brighter.

The integrated scatter over the angles we measured is about five times higher than the high-quality AR coatings on the enhanced LIGO viewports, measured here [4]. But still probably only ten to tens of ppm when all of the solid angle is taken into account.

Still, clearly the BRDF and TIS of the AR coating could be lower if whatever causes the leopard pattern were removed.

References

[1] GariLynn Billingsley, LIGO Document C1000474-v2, "ITM06 Input Test Mass Final Polishing Data Package," 2010. https://dcc.ligo.org/LIGO-C1000474

[2] GariLynn Billingsley, LIGO Document E1300886-v1, "ITM06 Figure Measurement," 2013. https://dcc.ligo.org/LIGO-E1300886

[3] GariLynn Billingsley and Laurent Pinard, LIGO Document C1103260-v1, "ITM06 Vendor Coating Characterization Report," 2011. https://dcc.ligo.org/LIGO-C1103260

[4] Cinthia Padilla, Peter Fritschel, Fabian Magaa-Sandoval, Erik Muniz, Joshua R. Smith, and Liyuan Zhang, "Low scatter and ultra-low reflectivity measured in a fused silica window," *Applied Optics*, Vol. 53, Issue 7, pp. 1315-1321 (2014). http://www.opticsinfobase.org/ao/abstract.cfm?uri=ao-53-7-1315

[5] F. Maganña-Sandoval, R. X. Adhikari, V. Frolov, J. Harms, J. Lee, S. Sankar, P. R. Saulson, and J. R. Smith, Large-angle scattered light measurements for quantum-noise filter cavity design studies, J. Opt. Soc. Am. 29, 17221727 (2012). http://www.opticsinfobase.org/josaa/abstract.cfm?uri=josaa-29-8-1722

[6] J. C. Stover, Optical Scattering, third edition (SPIE Press, 2012).